Journal of Power Sources 201 (2012) 408–412

Contents lists available at SciVerse ScienceDirect

Journal of Power Sources

journal homepage: www.elsevier.com/locate/jpowsour

Short communication

Enhanced photovoltaic performance of dye-sensitized solar cells using TiO_2-decorated ZnO nanorod arrays grown on zinc foil

Taibo Guo, Yiqing Chen*, Lizhu Liu, Yinfen Cheng, Xinhua Zhang, Qiang Li, Meiqin Wei, Baojiao Ma

School of Materials Science and Engineering, Hefei University of Technology, Hefei, Anhui 23009, PR China

ARTICLE INFO

Article history:
Received 31 July 2011
Received in revised form 30 October 2011
Accepted 31 October 2011
Available online 6 November 2011

Keywords:
ZnO nanorod arrays
TiO_2
Dye-sensitized solar cells
Zn foils

ABSTRACT

TiO_2-decorated ZnO nanorod arrays directly grown on zinc foil are fabricated by a two-step approach combining hydrothermal oxidation and a sol–gel process for dye-sensitized solar cells (DSSCs) applications. Its dye absorption and light harvesting are increased by decoration with a TiO_2 particle layer, resulting in enhancement of the photocurrent density. In addition, the open-circuit voltage (V_{OC}) of the DSSCs is improved by suppressing interfacial carrier recombination. As a result, the conversion efficiency (η) of the TiO_2-decorated ZnO photoanode is increased by a factor of 1.78 compared with that of the bare ZnO. The electrochemical impedance spectroscopy (EIS) analysis shows that depositing TiO_2 particles on the surface of the ZnO nanorod arrays can effectively extend electron lifetime and decrease electron recombination rate.

1. Introduction

Dye-sensitized solar cells (DSSCs), as a potential, cost-effective alternative to silicon solar cells, based on a dye-sensitized wide-band-gap nanocrystalline semiconductor (typically TiO_2 and ZnO) films have attracted widespread attention since they were first introduced by O'Regan and Grätzel in 1991 [1]. ZnO is a promising candidate for an alternative anode material, since it possesses an energy-band structure and physical properties similar to those of TiO_2, while it has higher electron mobility, lower combination rate, and better crystallization compared with TiO_2 [2,3]. Recently, DSSCs based on one-dimensional (1D) ZnO nanostructures, including nanowires and nanotubes, have begun to attract wide attention because of better electron mobility in 1D structures [4–6]. However, as photoanode materials, the poor adhesion between ZnO nanostructures and the *F*-doped SnO_2 (FTO) substrate is a key problem, which has limited the application of ZnO nanostructure in DSSCs. Although the adhesion can be improved by the annealing of the seed layer, it seems difficult to avoid peeling of the substrates in large-scale production [7]. In addition, ZnO-based DSCCs have disadvantages of the relative instability of ZnO when exposed to dye-loading solutions as ZnO readily reacts with dye molecules to form insulating complexes (Zn^{2+}/dye agglomerates), which may hinder electron injection from the dye molecules to the semiconductor [8]. One way to improve stability of ZnO-based DSCCs is to modify the surface chemistry via a coating layer. Moreover, the decorating layer is also believed to play a role in suppressing the recombination rate by passivating the recombination sites on the ZnO surface and by forming an energy barrier that prevents the injected electrons from approaching the nanowire surface [9,10].

To overcome the above limitations, a novel ZnO-based photoanode has been fabricated using zinc foil as a substrate instead of fluorine-doped SnO_2 (FTO) transparent conducting glass, and further modified by TiO_2 particles deposited on the surface of the ZnO nanorods for DSSC applications. The TiO_2-decorated ZnO (TiO_2/ZnO) nanorod arrays on flexible zinc foils have been fabricated by a two-step process, first giving a vertical ZnO nanorod arrays grown on zinc foil under hydrothermal condition, then followed by depositing TiO_2 particles on the surface of the ZnO nanorods using a sol–gel method. These cells have the advantages of low cost, simple preparation procedure, and naturally good adhesion between the ZnO nanorod arrays and the zinc foils. Furthermore, ohmic contact between the ZnO nanostructures and the zinc substrate facilitates electron transport and collection [11]. In addition, TiO_2 particles dispersed between ZnO nanorods can offer a high surface area for dye loading. The morphology, structures, and photoelectrochemical properties are characterized and studied in detail. The current–voltage results indicate that the solar conversion efficiency of DSSCs made using TiO_2 decoration is increased by a factor of 1.78, compared with those without TiO_2.

2. Experimental

2.1. Synthesis of TiO_2-decorated ZnO nanorod array electrodes

In a typical procedure [12], the clean zinc foils, as both the zinc source and the substrates, were immersed in a solution of

* Corresponding author. Tel.: +86 551 290 4636; fax: +86 551 290 1362.
E-mail address: chenyq63@126.com (Y. Chen).

0378-7753/$ – see front matter © 2011 Elsevier B.V. All rights reserved.
doi:10.1016/j.jpowsour.2011.10.114

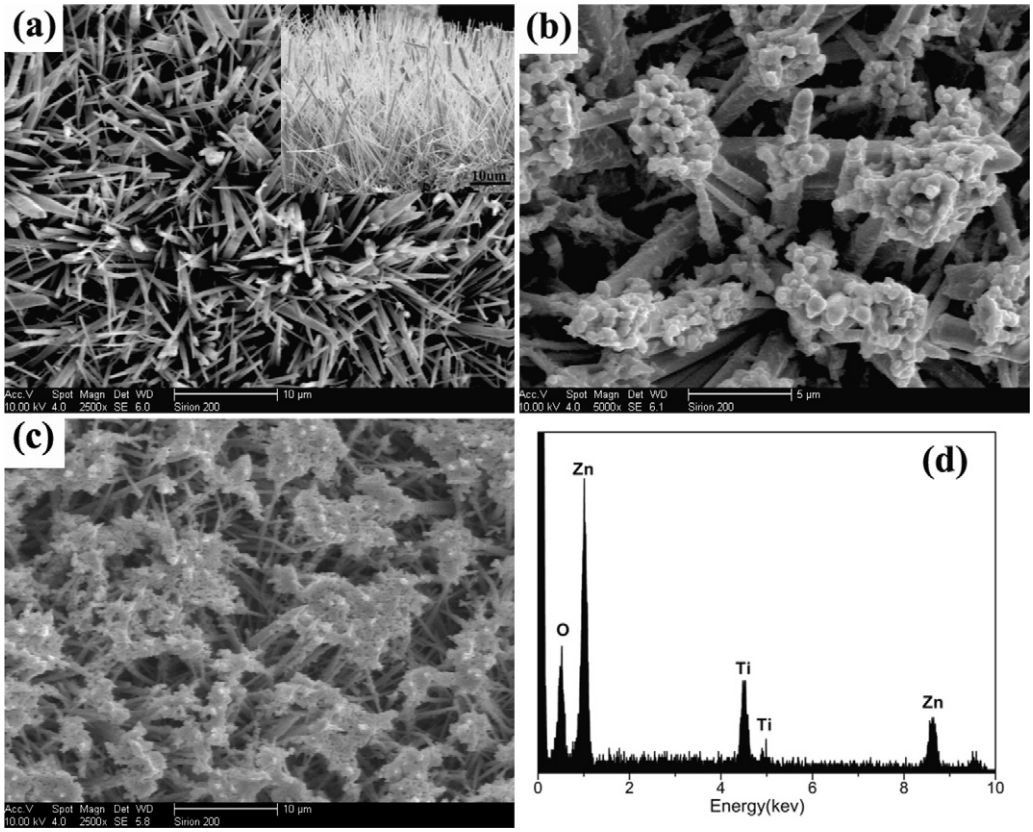

Fig. 1. (a) Top-view SEM image of the as-prepared ZnO nanorod arrays grown on a zinc foil. The inset is a side-view SEM image. (b) and (c) SEM images of TiO_2/ZnO nanostructures with dip-coating times of 10 cycles and 30 cycles, respectively. (d) Corresponding EDS pattern of the ZnO nanorods arrays after dip-coating times of 10 cycles.

ethylenediamine (12 mL), ethanol (10 mL) and water (13 mL). The solution was placed in a Teflon-lined stainless steel autoclave (50 mL), and was heated to, then maintained at a temperature of 170 °C for 20 h. The resulting zinc foils carrying ZnO nanorods were taken out and thoroughly rinsed with ethanol and dried in air. Subsequently, the surface of the ZnO nanorod arrays was decorated with TiO_2 particles by dipping in a well-dispersed TiO_2 sol (tetrabutyltitanate (0.2 M) in ethanol, modified with acetylacetone), water, and ethanol. Each dip-coating cycle took 10 s and each sample was given different number of cycles. The as-synthesized films were dried at 100 °C for 10 min, and heated to 450 °C for 2 h in air to obtain the TiO_2-decorated ZnO nanorod arrays.

2.2. Fabrication of DSSC

For DSSC fabrication, TiO_2-decorated ZnO nanorod array electrodes were immersed in a 0.3×10^{-3} mol L^{-1} ethanol solution of N719 (cis-diisothiocyanato-bis(2,20-bipyridyl-4,40-dicarboxylato) ruthenium(II) bis(tetrabutylammonium), Dalian HeptaChroma SolarTech, China) for 2 h for dye loading. The DSSCs were assembled by sandwiching the (Zn foils)/(dye-sensitized TiO_2/ZnO nanorod array anodes)/(Pt-coated FTO cathodes) using a frame of thermoplastic films (Surlyn™ 1702, Dalian HeptaChroma SolarTech, 25 μm thick) and were laminated for about 1 min at 125 °C. The internal space of the cell was filled with an electrolyte (0.5 M LiI, 50 mM I_2, 0.5 M 4-tertbutylpyridine in 3-methoxypropionitrile, Dalian HeptaChroma SolarTech) by capillary action through a small predrilled hole in the counter electrode. The total active electrode area was 0.20 cm^2.

2.3. Characterization and photoelectrochemical measurement

The morphology and the structure of the hybrid electrodes were characterized by field emission scanning electron microscopy (FESEM: FEI Sirion 200, USA) and X-ray diffraction (XRD: X'Pert PRO, PHILIPS). To study the composition, the sample was subjected to energy dispersive X-ray spectrum (EDS, Oxford INCA). The optical absorption spectra of the dye coated electrodes were measured by a UV–Vis-NIR spectrophotometer (DUV-3700, SHIMADZU, Japan). The photovoltaic performance of the DSCCs was measured by a Keithley 4200 under a solar simulator (XES-301S, NIPPON SOKKI, Xenon lamp, AM 1.5, 100 mW cm^{-2}), and the incident light intensity was calibrated with a standard crystalline silicon solar cell. Electrochemical impedance spectra (EIS) were measured using an electrochemical work station (CHI660D, CH Instruments, Shanghai) at V_{OC} with a bias alternating current (AC) signal of 5 mV in the frequency range of 1–10^5 Hz.

3. Results and discussion

The morphology of the ZnO nanorod arrays grown on a zinc foil substrate is shown in Fig. 1a. The nanorod arrays are of diameters ranging from 200 to 500 nm and lengths of about 15 um (from the side view of inset). The surface of the nanorods is smooth, and aligned ZnO nanorods directly grow on the Zn substrate. It can be observed that a large number of particles are coated on the surfaces of ZnO nanorods after 10 cycles of dip-coating, as shown in Fig. 1b. With 30 cycles of dip-coating many more particles penetrated and were dispersed between the ZnO nanorods, with the larger fraction coating the top surface of the arrays (Fig. 1c). The EDS spectrum (Fig. 1d) indicates that the nanorod arrays are composed of the elements Zn, Ti, and O after 10 cycles of dip-coating.

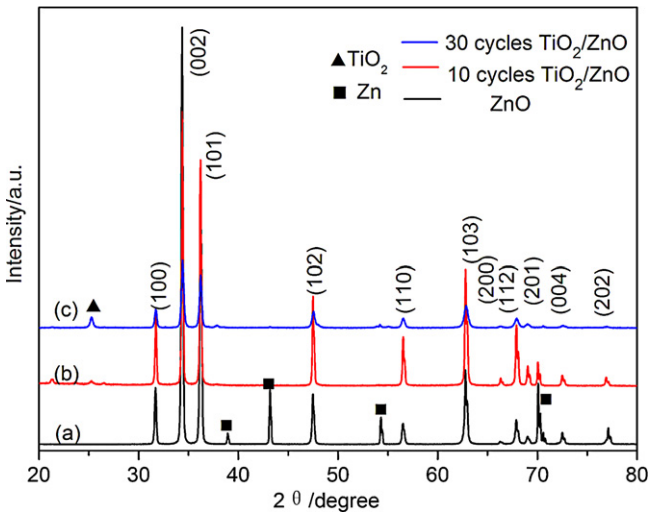

Fig. 2. XRD spectra of the original ZnO nanorod arrays (a) and the TiO_2/ZnO nanostructures with different dip-coating cycles ((b) and (c)) on zinc foil.

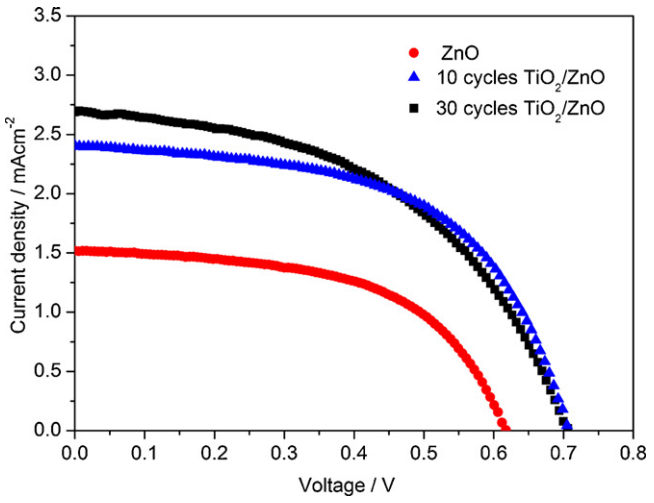

Fig. 4. The *J–V* characteristics of DSSCs with ZnO and TiO_2 decorated ZnO electrodes under 1 sun (AM 1.5 G) illumination.

The X-ray diffraction pattern (Fig. 2) shows that the initial ZnO nanorod arrays has a strong and sharp (0 0 2) diffraction peak, indicating the oriented growth of good crystalline nanorods along the *c*-axis direction, which is in good agreement with the standard pattern (JCPDS 36-1451). It is clear that TiO_2 shows a peak corresponding to the anatase (1 0 1) dominant peak (25.2°, JCPDS 21-1272), and the (1 0 1) reflection apparently predominates at dip-coating times from 10 to 30 cycles (curves *b* and *c*) after annealing at 450 °C. In addition, Zn diffraction peaks appear from the zinc substrate.

To understand the influence of light absorption with ZnO electrodes decorated by TiO_2, ultraviolet–visible (UV–Vis) absorption measurements were performed. Fig. 3 shows the UV–Vis absorption spectra of the ZnO and TiO_2/ZnO nanorod arrays with and without sensitization by N719 dye. It can be observed that the band gap absorption edge of the ZnO/TiO_2 sample (curve *b*) is red-shifted compared with that of ZnO (curve *a*), which may be attributed to the narrower band gap of TiO_2 compared with that of ZnO [13,14]. Therefore, the TiO_2/ZnO composite films extend the photo-response into the visible spectrum, which means that it improves the utilization efficiency of visible light. After dye-sensitization, both the ZnO and TiO_2/ZnO nanorod arrays (curves *c* and *d*) present absorption peaks centered around 520 nm, which correspond to the intrinsic peak of the N719 dye absorbed on the surface of the ZnO and TiO_2/ZnO nanorod arrays. It may be clearly seen that the TiO_2/ZnO nanorod arrays shows a higher absorption than that of the bare ZnO nanorod arrays for the same sensitization time in the range of 450–720 nm, which may result from the higher surface area and the higher light harvesting properties of TiO_2-decorated materials.

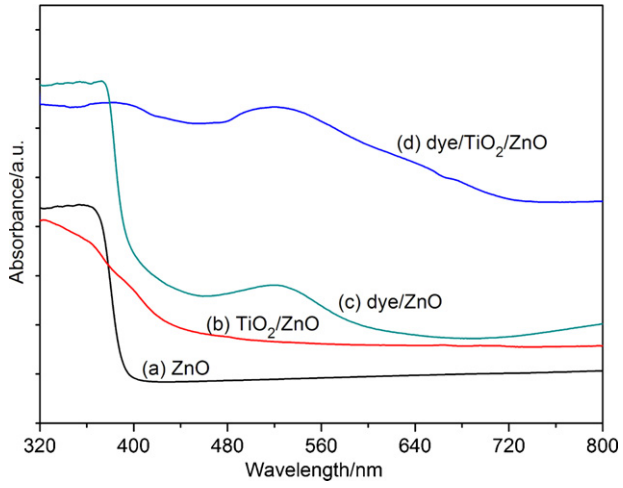

Fig. 3. Ultraviolet–visible (UV–Vis) absorption spectra of (a) ZnO, (b) TiO_2/ZnO, (c) dye-sensitized ZnO, (d) dye-sensitized TiO_2/ZnO on Zn foil.

Fig. 4 shows the comparison of photocurrent–voltage (*J–V*) characteristics for the cells fabricated using the bare ZnO nanorod arrays and TiO_2-decorated ZnO nanorod arrays on Zn foils. The corresponding photovoltaic parameters of the DSSCs are summarized in Table 1. It can be seen that the short-circuit photocurrent (J_{SC}) density of DSSCs increases with an increasing amount of TiO_2 particles, due to the increment of dye absorption by TiO_2/ZnO compared to that by bare ZnO, which allows more injection of photogenerated electrons, in conformity with the above result from Fig. 3. In fact, the J_{SC} of our device is underestimated because the incident light is diminished by the Pt layer on the counter electrode [15]. The open-circuit photovoltage (V_{OC}) is also increased by 14%, which can be explained by inhibition of the back electron transfer from the conduction band of ZnO to the dye cations and/or I^{3-} ions, or in other words, the suppression of interfacial charge recombination due to TiO_2 decorating [16]. The power conversion efficiency was calculated using the following equations:

$$FF = \frac{J_{max}V_{max}}{J_{SC}V_{OC}} \quad (1)$$

$$\eta = \frac{J_{SC}V_{OC}FF}{P_{in}} \quad (2)$$

For Eq. (1), *FF* is the fill factor; P_{in} is the energy of the incident light (100 mW cm^{-2}). J_{max} (mA cm^{-2}) and V_{max} (V) are the current density and voltage at the point of maximum power output in the *J–V* curve, respectively. The TiO_2/ZnO-based DSSCs (10

Table 1
Performances parameters of DSSCs with ZnO and TiO_2/ZnO film photoanodes measured using a solar simulator under one sun illumination (100 mW cm^{-2}).

Electrodes	V_{OC} (V)	J_{SC} (mA cm^{-2})	*FF* (%)	η (%)
ZnO	0.618	1.52	56	0.53
10-cycle TiO_2/ZnO	0.706	2.41	55	0.94
30-cycle TiO_2/ZnO	0.707	2.69	49	0.93

V_{OC}, open-circuit voltage; J_{SC}, short-circuit photocurrent density; *FF*, fill factor; η, overall conversion efficiency.

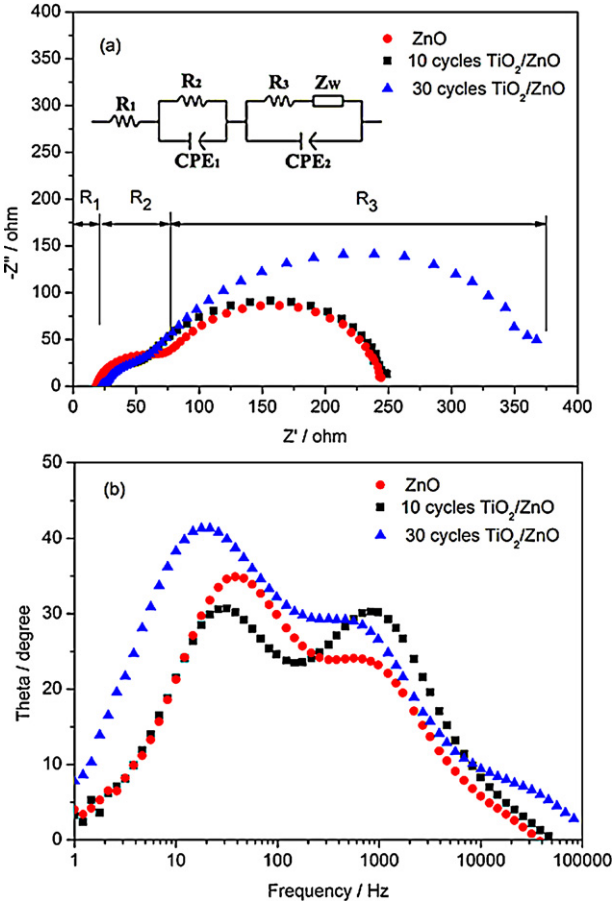

Fig. 5. Electrochemical impedance spectroscopy (EIS) results (Nyquist plot (a) and Bode phase plots (b)) of different electrodes at open circuit voltage in AM 1.5 G illumination. The equivalent circuit is shown in the inset of (a).

cycles) exhibit a maximum light to electricity conversion efficiency (η) of 0.94% with a fill factor of 55%, a short-circuit current of 2.69 mA cm^{-2} and an open-circuit voltage of 0.707 V. From the results as shown in Table 1, the conversion efficiencies of DSSCs using 10-cycles TiO_2/ZnO composites are increased by a factor of 1.78 compared with those using ZnO alone. This demonstrates the merits of using a decorating layer of TiO_2 particles at the ZnO/electrolyte interface, which is associated with the higher light harvesting properties of TiO_2-decorated materials. The fill factor (*FF*) is known to be determined by the series resistance of the cell, including the resistances of the Zn foil, the photoelectrode, the electrolyte, and the counter electrode. Here, the *FF* decreased from 0.56 to 0.49, which may be attributed to the larger series resistance after decorating by TiO_2 particles. It is noteworthy that the energy conversion efficiency for a 10-cycle preparation TiO_2/ZnO is not high compared with figures given elsewhere [10], an important reason for which is that the incident light is obviously diminished under back illumination from the side of Pt-coated/FTO. Nevertheless, this construction and its applications to DSSC can be a good reference for future research work. To further elucidate the role of TiO_2 in the charge transfer properties of TiO_2/ZnO electrode-based DSSCs, an AC impedance measurement (Nyquist plots and Bode plots) was performed in an electrochemical impedance system.

Electrochemical impedance spectroscopy (EIS), which provides the information of capacitance and resistance of the electrode materials, is an effective approach for investigating electron transfer across the electrolyte and the surface of the electrode [17–19]. Fig. 5 illustrates the typical impedance spectra (Nyquist plots and Bode plots) of the bare ZnO electrode and TiO_2/ZnO electrodes with different decorating cycles at an AC frequency varying from 100 kHz to 1 Hz. Generally, the Nyquist plot for DSCCs usually consists of three semi-circles: the redox reaction at the platinum counter electrode/electrolyte interface at high frequency (R_2), the electron transfer at the photoanode/electrolyte interface at medium frequency (R_3) and carrier transport by ions in the electrolyte at low frequency. However, the EIS test in this study is terminated after the second semicircle as this circle is directly related to charge transfer at the TiO_2 photoanode/electrolyte interface [20,21]. As shown in Fig. 5a, semicircle diameters R_2 and R_3 are the charge transfer resistances at the corresponding interfaces, while R_1 is ohmic, mainly caused by the sheet resistance of the Zn foils. Reductions or increases in the impedance should be correlated with an increase or decrease, respectively, in the electron drift mobility through the electrode. An equivalent circuit shown in the inset of Fig. 5a is employed to fit the impedance data, using Zsimpwin impedance analysis software (Version 3.10, by Echem). CPE (constant phase element) is a nonideal frequency dependent capacitance, a characteristic that can be associated with a distribution of relaxation times or with a nonuniform distribution of current due to material heterogeneity. Z_W relates to the Warburg diffusion of the redox species within the I^-/I^{3-} electrolyte [22]. It is obvious that the charge transfer resistance assigned to the electron transfer at the dye-absorbed photoanode/electrolyte interface (as denoted as R_3 in Fig. 5a) increased with the introduction of TiO_2 layer [23]. Moreover, the series resistance R_1 is also increased, which may be one of the crucial reason for the low *FF* after 30-cycles decoration [24].

One can observe two phase angle peaks in the Bode plot (Fig. 5b) that correspond to two semicircles in the Nyquist plot (Fig. 5a). The electron lifetime (τ) is estimated from the following relationship: $\tau \approx 1/\omega_{max} = 1/2\pi f_{max}$, where f_{max} is the maximum frequency of the medium frequencies peak (10–100 Hz) [25]. From the medium-frequency peak in the Bode plots, it can be seen that the frequency peak of TiO_2/ZnO-based DSSCs is shifted to lower frequency compared with that of a ZnO-based DSSC. Correspondingly, the electron lifetime is calculated to be 4.1, 5.0 and 9.0 ms for the three cells, respectively. The longer lifetime implies a lower recombination rate and an enhanced electron-collection efficiency. Therefore the interfacial charge recombination of ZnO between the photo-injected electron and electrolyte materials is reduced after the TiO_2 decoration. This consequently leads to a significantly enhanced energy conversion efficiency of the cell.

4. Conclusions

In summary, a simple and rapid method is demonstrated that Zn foils may be used as a collecting anode in a DSSC to provide good adhesion and for direct growth of a ZnO nanorod array. TiO_2-decorated ZnO nanorod arrays directly grown on zinc foil are successfully prepared by a two-step approach combining hydrothermal oxidation and a sol–gel process. The influence of TiO_2-decorated layer on the photovoltaic properties of ZnO-based DSSCs is also investigated. The results show that TiO_2 particles layers provide an intrinsic energy barrier which effectively suppresses charge recombination and increases the electron lifetime. At the same time, TiO_2/ZnO nanorod arrays with higher surface area have higher dye loading and higher light harvesting compared with that of a bare ZnO film. The optimized decoration of TiO_2 particles improves the performance of the TiO_2/ZnO-based DSSCs.

Acknowledgement

This work was financially supported by the Natural Science Foundation of China (NSFC, No. 21071039).

References

[1] B. O'Regan, M. Grätzel, Nature 353 (1991) 737–740.
[2] C. Longo, M.-A. De Paoli, J. Braz. Chem. Sci. 14 (2003) 889–901.
[3] M. Quintana, T. Edvinsson, A. Hagfeldt, G. Boschloo, J. Phys. Chem. C 111 (2007) 1035–1041.
[4] I.G. Valls, Y. Yu, B. Ballesteros, J. Oro, M.L. Cantu, J. Power Sources 196 (2011) 6609–6621.
[5] A.B.F. Martinson, J.W. Elam, J.T. Hupp, M.J. Pellin, Nano Lett. 7 (2007) 2183–2187.
[6] M. Law, L.E. Greene, J.C. Johnson, R. Saykally, P.D. Yang, Nat. Mater. 4 (2005) 455–459.
[7] J. Chung, J. Lee, S. Lim, Physica B 405 (2010) 2593–2598.
[8] K. Keis, C. Bauer, G. Boschloo, A. Hagfeldt, K. Westermark, H. Rensmo, H. Siegbahn, J. Photochem. Photobiol. A 148 (2002) 57–64.
[9] M. Law, L.E. Greene, A. Radenovic, T. Kuykendall, J. Liphardt, P.D. Yang, J. Phys. Chem. B 110 (2006) 22652–22663.
[10] Q.F. Zhang, C.S. Dandeneau, X.Y. Zhou, G.Z. Cao, Adv. Mater. 21 (2009) 4087–4108.
[11] Y. Jiao, H.J. Zhu, X.F. Wang, L. Shi, Y. Liu, L.M. Penge, Q. Li, Cryst. Eng. Comm. 12 (2010) 940–946.
[12] Y.X. Wang, X.Y. Li, G. Lu, X. Quan, G.H. Chen, J. Phys. Chem. C 112 (2008) 7332–7336.
[13] Y.Z. Lei, G.H. Zhao, M.C. Liu, Z.N. Zhang, X.L. Tong, T.C. Cao, J. Phys. Chem. C 113 (2009) 19067–19076.
[14] C.W. Zou, X.D. Yan, J. Han, R.Q. Chen, J.M. Bian, E. Haemmerle, W. Gao, Chem. Phys. Lett. 476 (2009) 84–88.
[15] Z.Z. Yang, T. Xu, Y. Ito, U. Welp, W.K. Kwok, J. Phys. Chem. C 113 (2009) 20521–20526.
[16] K.E. Kim, S.-R. Jang, J. Park, R. Vittal, K.-J. Kim, Sol. Energy Mater. Sol. Cells 91 (2007) 366–370.
[17] T.V. Nguyen, H.C. Lee, O.B. Yang, Sol. Energy Mater. Sol. Cells 90 (2006) 967–981.
[18] J. Van de Lagemaat, N.G. Park, A.J. Frank, J. Phys. Chem. B 104 (2000) 2044–2052.
[19] J. Bisquert, G. Garcia-Belmonte, F. Fabregat-Santiago, N.S. Ferriols, P. Bogdanoff, E.C. Pereira, J. Phys. Chem. B 106 (2002) 325–333.
[20] Q. Wang, J.E. Moser, M. Grätzel, J. Phys. Chem. B 109 (2005) 14945–14953.
[21] F.F. Santiago, J. Biquert, G.G. Belmonte, G. Boschloo, A. Hagfeldt, Sol. Energy Mater. Sol. Cells 87 (2005) 117–131.
[22] C.P. Hsua, K.M. Lee, J.T.W. Huang, C.Y. Lin, C.H. Lee, L.P. Wang, S.Y. Tsai, K.C. Ho, Electrochim. Acta 53 (2008) 7514–7522.
[23] K. Park, Q.F. Zhang, B.B. Garcia, G.Z. Cao, J. Phys. Chem. C 115 (2011) 4927–4934.
[24] T. Hoshikawa, M. Yamada, R. Kikuchi, K. Eguchi, J. Electrochem. Soc. 152 (2005) 68–73.
[25] R. Kern, R. Sastrawan, J. Ferber, R. Stangl, J. Luther, Electrochim. Acta 47 (2002) 4213–4225.